Scripta Materialia 161 (2019) 40–43

Contents lists available at ScienceDirect

Scripta Materialia

journal homepage: www.elsevier.com/locate/scriptamat

Regular article

Segregation of $Al_{1.5}CrFeNi$ high entropy alloys induced by vacancy-type defects

Sen Sun [a], Nan Qiu [a], Kun Zhang [a], PingNi He [a], YongJun Ma [b], FuJun Gou [a,*], Yuan Wang [a,c,*]

[a] Key Laboratory of Radiation Physics and Technology, Ministry of Education, Institute of Nuclear Science and Technology, College of Physical Science and Technology, Sichuan University, Chengdu 610064, PR China
[b] Analysis & Testing Center, Southwest University of Science and Technology, Mianyang 621010, PR China
[c] Key Laboratory of Nuclear Materials and Safety Assessment, Chinese Academy of Sciences, Shenyang 110016, PR China

ARTICLE INFO

Article history:
Received 28 September 2018
Accepted 10 October 2018
Available online 17 October 2018

Keywords:
Vacancy-induced segregation
RIS tolerance
High entropy alloy films
Vacancy-type defects
Atomic size

ABSTRACT

The radiation-induced segregation (RIS) of high entropy alloys (HEAs) have gained significant interest, however, the RIS mechanisms are not fully elucidated, mostly due to the inability to resolve the complexity of the effects of vacancies and interstitials on the alloying elements of HEAs. In this work, we investigated the effects of single vacancy-type defects on the segregation of $Al_{1.5}CrFeNi$ films. The results show that vacancy-type defects can induce significant segregation on the $Al_{1.5}CrFeNi$ alloys; vacancy-induced segregation evolution of HEAs depend on the atomic size of the alloy elements, in which oversized atoms diffusing faster while undersized atoms diffusing slower.

High-entropy alloys (HEAs) are novel materials composed of four or more principal elements in equal or near-equal atomic ratio that form single-phase solid solutions [1], which provide some excellent properties, such as high strength, high temperature thermal stability, ductility, improved fracture toughness and corrosion resistance due to the extreme compositional complexity and inherent lattice distortions [1–3]. Therefore, HEAs are expected to be candidates for next-generation advanced nuclear reactors as structural and functional applications under harsh operating environments.

Multiple systems of HEAs have been investigated under irradiation conditions and exhibited excellent radiation tolerance [4–6]. In particular, recent studies have found that HEAs exhibit enhanced radiation-induced segregation (RIS) tolerance compared to stainless steels or single principal element alloys [3,4,7,8]. Nonetheless, there is practically nothing known about their intrinsic RIS mechanism. Prior extensive RIS investigation has been done on alloys with one or two principal elements. It is confirmed that RIS is an enhanced diffusion of components of alloys in local irradiation zone under the effect of rapidly migratory point defects (vacancies and interstitials), leading to enrichment or depletion of alloy elements near sinks in the irradiated materials [9–14]. However, it should be noted that the migration rate of vacancies and interstitial atoms is different [5], and the interaction mechanism between the two types of point defects and alloying elements is also different [15,16]. Obviously, the vacancies and interstitial atoms can inevitably have different effects on RIS behavior of the irradiated materials. The complexity of the effects of these two defects on the segregation behavior of alloying elements would makes it difficult to understand the RIS nature of the materials, especially for HEAs with complex components. In this regard, it is necessary to investigate specifically the RIS behavior of HEAs under the interaction between single-type defects and the alloy elements for further exploring RIS tolerance mechanism of HEAs. Hereby, we chose a plasma surface interaction (PSI) facility which can release low-energy and high-fluence ion irradiation to produce a large number of vacancy-type defects on the surface of the irradiated HEAs. In general, the interstitial atoms generated by the PSI mainly accumulate on the surface of the materials, and easily move from the surface of materials by overcoming surface energy, resulting in an abnormal accumulation of oversaturated vacancy-type point defects on the surface of the irradiated materials [17,18]. Then, a large amount of vacancy fluxes can be formed from the surface to the bottom of the irradiated samples due to an existence of vacancy concentration gradient.

In the current work, single phase $Al_{1.5}CrFeNi$ HEA films were prepared and irradiated at different fluences for investigating the RIS behavior of the HEAs under effect of vacancy-type defects produced by the PSI facility. We observed that the number of helium bubbles decreased along the depth of the films and oversized Cr-atoms segregated on the surface while undersized Ni-atoms segregated at the bottom of the irradiated film. The results reveal that single vacancy-type defects can induce alloying elements segregation in the $Al_{1.5}CrFeNi$ HEA films,

* Corresponding authors at: Key Laboratory of Radiation Physics and Technology, Ministry of Education, Institute of Nuclear Science and Technology, College of Physical Science and Technology, Sichuan University, Chengdu 610064, PR China.
E-mail addresses: gfujun@scu.edu.cn (F. Gou), wyuan@scu.edu.cn (Y. Wang).

https://doi.org/10.1016/j.scriptamat.2018.10.014
1359-6462/

and vacancy-induced segregation behavior is sensitive to the atomic size of the components in the $Al_{1.5}CrFeNi$ HEAs.

$Al_{1.5}CrFeNi$ high-entropy alloy films were deposited on Si (100) single crystal substrates by using a radio frequency (RF) magnetron sputtering system with a base pressure of 5×10^{-4} Pa and an RF power of 100 W. An aluminum plate (99.999%, purity) with several circular chromium, iron and nickel sectors on it (99.99% in purity and 1 mm in thickness) was used as a target. The thickness of the deposited thin films was kept about 1 μm. All films were deposited to a nominal thickness of 1 μm. Some samples were annealed from 773 K to 1173 K in an ultra-high vacuum furnace pumped to 1.2×10^{-4} Pa for 1 h, while the others were irradiated using 80 eV He+ with fluences ranging from 6×10^{18} to 1.8×10^{21} cm^{-2} under a 5 Pa Helium atmosphere in a plasma surface interaction (PSI) facility. Compared with routine irradiation, PSI has following characteristics: low ion irradiation energy, high ion fluence and high surface temperature, which make the interstitials sputtering effects on the surface of the materials more significant [17], leading to a huge difference of irradiation environment compared with routine irradiation. The base pressure of the PSI facility was 3×10^{-2} Pa. The ion fluxs were kept at 1×10^{17}–1×10^{18} cm^{-2} s^{-1} for the irradiated samples. The temperature of the sample measured by a thermocouple connected to the substrate during irradiating was about 773 K, 873 K and 973 K because of the different He+ ion fluences, respectively. The predicted damage range of the irradiated films was about 3 nm as calculated by using SRIM 08, and only Al atoms left the lattice to become interstitials under helium ion bombardment. In fact, a large amount of Al atoms could also be sputtered out of the surface of the films during irradiating [17,19,20]. Grazing incidence (2.0°) X-ray diffraction (GIXRD, Philips X Pert Pro MPD DY129) measurements were performed to ascertain the crystallographic structure of the films by using a diffractometer with Cu-Kα radiation source. A transmission electron microscope (TEM) and scanning transmission electron microscope (STEM, Zeiss Libra200FE) with an energy-dispersive spectrometer (EDS) operated at 200 keV was employed for TEM bright field (TEM-BF) imaging, high angle annular dark field (HAADF) imaging and analyzing chemical compositions of the $Al_{1.5}CrFeNi$ HEAs films. TEM foils from the as-deposited and the irradiated films were prepared by mechanical polishing to approximately 50 μm thickness, followed by ion milling (Leica EM RES101) to no more than 200 nm.

Fig. 1 shows the GIXRD patterns of the films irradiated with different He+ fluences and the films annealed at different temperature, respectively. The as-deposited $Al_{1.5}CrFeNi$ HEA film has a typical BCC structure which was broken down with the increase of the irradiation fluences as shown in Fig. 1a. The intensity of BCC diffraction peaks of the irradiated films decreased dramatically and could hardly be identified in the profile as the films were irradiated with the He+ ion fluence raised from 6×10^{18} cm^{-2} at 773 K to 1.8×10^{21} cm^{-2} at 973 K. However, the crystal structure of the annealed $Al_{1.5}CrFeNi$ films still remained stable even though the annealing temperature reached to 1173 K as shown in Fig. 1b. In general, the solid-state phase transformation of materials can be induced either or both by ion irradiation and high temperature annealing. Therefore, it can be concluded that the He ion irradiation rather than the high temperature played an important role in the phase transformation of the irradiated films in this work.

The HAADF and TEM-BF images of the cross-section of the as-deposited film and the irradiated films are shown in Fig. 2. The results show that the as-deposited and the films irradiated with the fluence of 6×10^{18} cm^{-2} were composed of columnar grains. No obvious defects are found in the samples as shown in Fig. 2a and b. However, A large number of dark spots appeared along the depth of the film with the increasing of the irradiation fluences as shown in Fig. 2c. The number and size of these dark spots (marked by white arrows) decreased along the depth of the $Al_{1.5}CrFeNi$ HEA film. This is exactly the same as the observed helium bubbles in TEM-BF image as shown in the inset image of Fig. 2(c3). Moreover, a large number of helium bubbles bursted into hollow fragments (marked by blue line) and some larger visible holes (marked by yellow ellipses or circles in Fig. 2d) can be even found at the bottom of the irradiated film with the further increasing irradiation fluence. It indicated that the oversaturated vacancies of the irradiated film had a strong downward diffusivity because the formation of helium bubbles is a combination of vacancy-type defects and helium atoms [21,22]. Moreover, the diffusion of the vacancies and helium even passed over the irradiated region of the films.

The results of EDS-mapping measurements along the cross-section of the as-deposited film and the irradiated films are also shown in Fig. 2. The distribution of alloy elements in the as-deposited and the films irradiated with the fluence of 6×10^{18} cm^{-2} was relatively uniform. No obvious element segregation can be found as shown in Fig. 2(a2) and (b2). However, the total content of Al in the whole irradiated film decreased continuously from 32% atomic ratio of the as-deposited film (Fig. 2(a1)) to 9% of the film irradiated with the fluence of 6×10^{19} cm^{-2} as shown in Fig. 2(c1). Only Al atoms could be knocked out of the lattice and the implanted depth of the incident He+ ions was very shallow according to the SRIM. Therefore, it is reasonable to believe that the reduction of Al in the whole film was resulted from Al sputtering which contributed most of vacancy-type point defects,

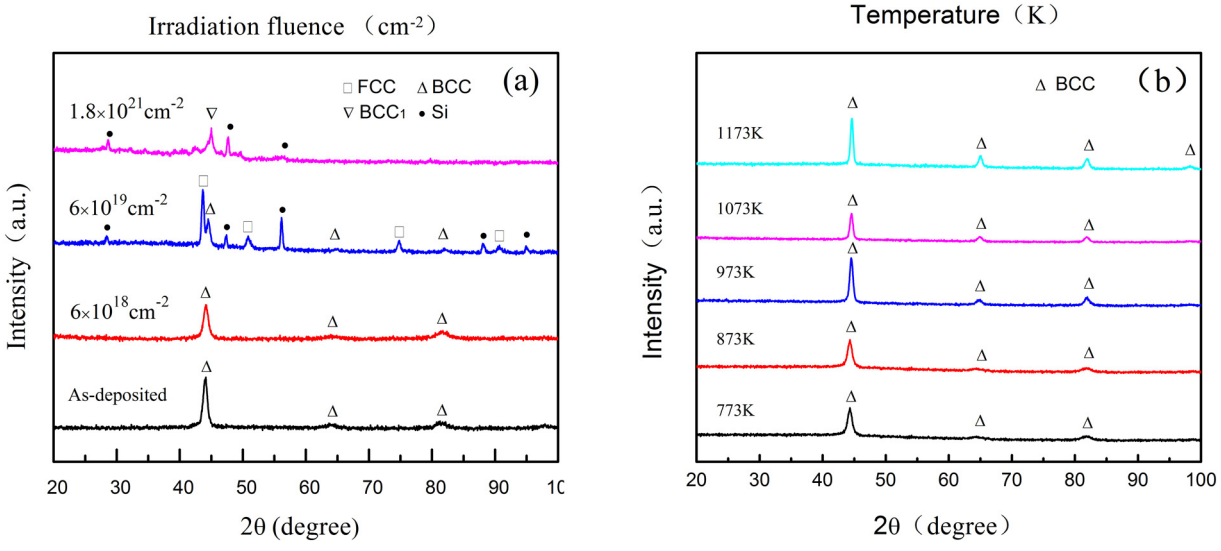

Fig. 1. GIXRD patterns of the $Al_{1.5}CrFeNi$ HEA films: (a) the films exposed to different irradiation fluences. (b) The films annealed at different temperature.

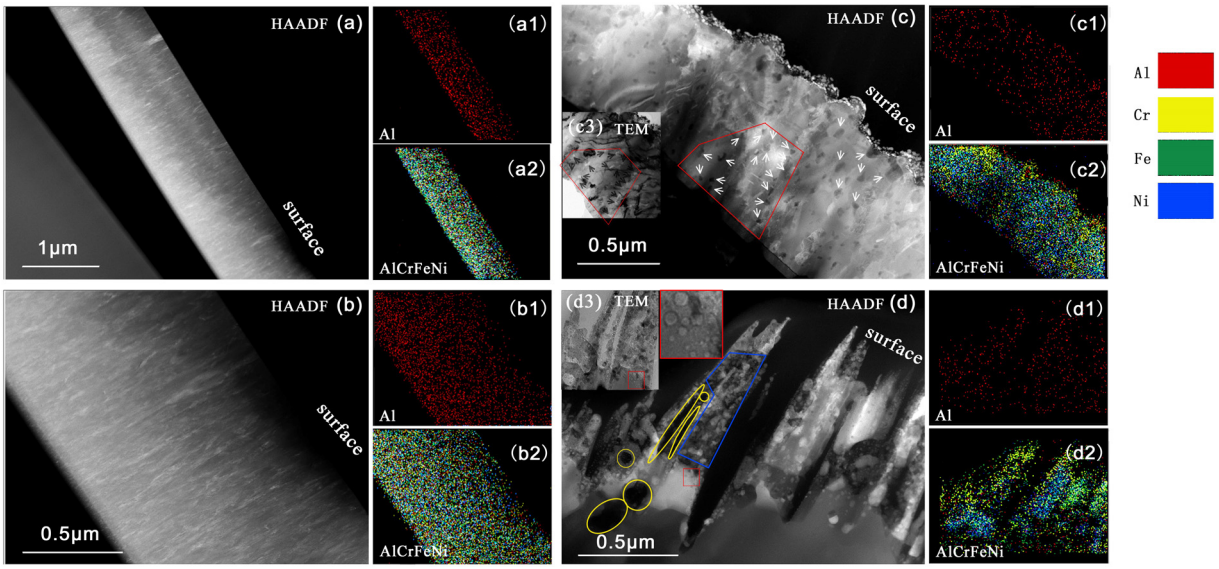

Fig. 2. HAADF and EDS/mapping images of the as-deposited and irradiated $Al_{1.5}CrFeNi$ films. HAADF images of the as-deposited film (a) and the irradiated film (b) to fluence of 6×10^{18} cm^{-2} at 773 K had no obvious defects. EDS/mapping of (a2) and (b2) had no obvious element segregation. HAADF image of the irradiated film (c) to fluence of 6×10^{19} cm^{-2} at 873 K had obvious helium bubble (marked by white arrows) distribution along the section of the film. HAADF image of the irradiated film (d) to fluence of 1.8×10^{21} cm^{-2} at 973 K had helium bubbles (marked by red square) and hollow fragments (marked by blue line) and holes (marked by yellow ellipses or circles) in the interior and at the bottom of the film. Al reduced by 72% in (c1) and Cr segregated on the surface of the irradiated film in (c2). A significant segregation of the alloy elements is also be found in (d2), in which the Cr segregated on the surface of the irradiated film, the Fe in the middle and the Ni at the bottom of the irradiated film, respectively.

making Al below the irradiated region (subsurface 3 nm) diffused upward to the surface of the irradiated film.

A remarkable segregation of the alloy elements except Al, however, is found in the irradiated film, in which Cr segregated on the surface, Fe in the middle and Ni at the bottom of the irradiated film as shown in Fig. 2(d2), respectively. Fig. 3 shows the further EDS measurements along the cross-section of the film (point 1 to point 7 in inserted HAADF image) irradiated with the fluence of 1.8×10^{21} cm^{-2}. Al had a low total content because of a synergy of the ion irradiation sputtering effect and itself diffusion, and its distribution was thus relative smooth in the irradiated film. However, the most alloy elements of the irradiated film exhibited a nonuniform distribution. For example, the Fe content reached up to 46% in the middle and decreased to 25% on both sides of the irradiated film, respectively. The RIS behavior of Cr and Ni nevertheless followed a completely opposite trend. The Cr content was firstly up to 68% on the surface and then decreased near zero at the bottom of the irradiated film, while the Ni content was 5% at the surface and 70% at the bottom of the irradiated film, respectively. It implied that the RIS below the irradiated region of the film might be caused by the downward diffusion of the defects in the irradiated region.

The defects produced by the routine irradiation conditions contain usually the same numbers of the vacancies and the interstitials. Therefore, the RIS is generally considered as a coupling between the fluxes of radiation induced vacancies and interstitial atoms toward these sinks and the fluxes of solutes in irradiated materials [9]. Marwick explained the RIS in austenitic steels by a coupling between the fluxes of the vacancies and the solute atoms, in which the undersized solute was a slow diffuser and the oversized solute was a rapid diffuser [15]. However, Okamoto et al. proposed that the undersized solutes were easy to form dumbbell configurations with the interstitials and transported by the interstitials to the sinks [16]. If the RIS of the irradiated films in this work was controlled by the interstitial-type point

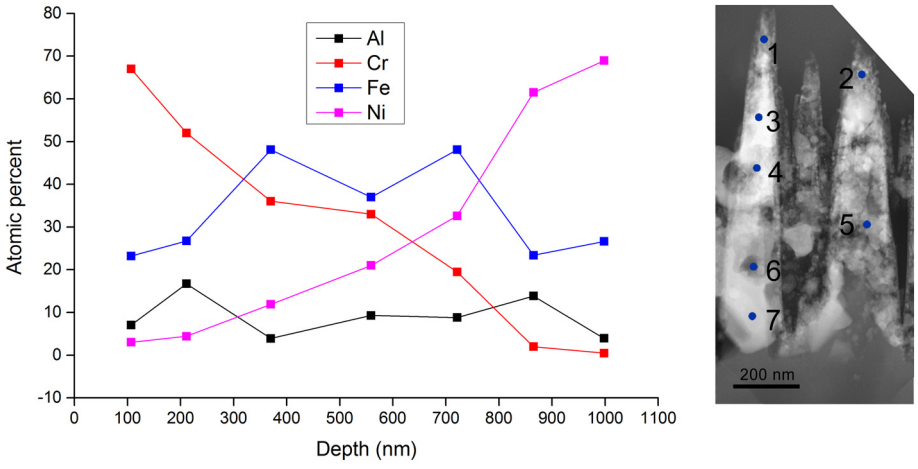

Fig. 3. The depth dependence of element content in the film irradiated with the fluence of 1.8×10^{21} cm^{-2}. Al had a low total content and Fe content reached up to 46% in the middle and decreased to 25% on both sides of the irradiated film. The RIS of Cr and Ni nevertheless followed a completely opposite trend. The Cr content was firstly up to 68% at the surface and then decreased near zero at the bottom of the irradiated film, while the Ni content was 5% at the surface and 70% at the bottom of the irradiated film. The inserted HAADF image shows the position of EDS measurements along the section of the irradiated film (point 1 to point 7).

Table 1
Atomic radius R of all relevant elements [23].

Element	Al	Cr	Fe	Ni	Mn	Co
R (pm)	119.9	112.8	109.1	107.7	118.0	108.9

defects, the undersized Ni in Table 1 [23] would be easier to form a dumbbell configuration with the interstitial Al and transported to the sinks by the interstitial. Thus, the Ni would be depleted at the bottom of the irradiated film because of the depletion of Al at the same place. However, it was not in agreement with the RIS result of the irradiated HEA films. It also implied that the vacancies mainly produced by the interstitial Al sputtering could have considerable effects on the RIS behavior of the irradiated film.

It is interesting that the oversized atoms can move faster than the undersized atoms under the vacancy-solute exchange mechanism in alloys due to the effect of bonding characteristics of the *d* electrons [24], despite the traditional view is that the larger the atom, the slower its diffusion rate [25]. The result of the measured diffusion coefficients of components in CoCrFeMnNi HEAs was $D_{Mn} > D_{Cr} > D_{Fe} > D_{Co} > D_{Ni}$, which confirmed the effects of the atom size on diffusion were applicable to HEAs [26]. It is clear from the above-mentioned discussion that, due to the different vacancy concentration, the oversaturated vacancies could diffuse downward from the irradiated region to the non-irradiated region. The opposite direction of the element diffusion fluxes was formed simultaneously under the vacancy-solute coupled exchange mechanism [15]. The oversized element Al (below the subsurface 3 nm irradiated region) as the fastest diffuser diffused upward to the irradiation region continuously, and then was sputtered out of the film, resulting in a significant decrease in Al content of the whole film (in Fig. 3). The oversized element Cr as the second fast diffuser segregated at the surface, while the undersized element Fe as the slower diffuser and Ni as the slowest diffuser segregated in the middle and at the bottom of the irradiated $Al_{1.5}$CrFeNi film, respectively. It indicated that the interaction of the vacancy-type defects and the elements determined the RIS behavior of the HEA films, moreover, the vacancy-induced segregation behavior depend on the atomic size of the alloy elements, in which oversized atoms diffusing faster while undersized atoms diffusing slower.

In summary, the effects of single vacancy-type defects on RIS behavior of the $Al_{1.5}$CrFeNi HEA films were investigated. The results indicate that dominating vacancy diffusion fluxes can be formed when the HEA materials were exposed to high-fluences irradiation environment. The alloying elements segregation of HEAs can be thus significantly induced by the interaction of the vacancies and the elements of the HEAs. Moreover, the vacancy-induced segregation of the irradiated HEAs is controlled intrinsically by the atomic size of the components in the HEAs. It can result in degradation of the material's properties, and thus shorten the service time of materials in the nuclear reactor. Therefore, selecting alloy elements with suitable atomic size may be an effective approach in designing RIS tolerant HEA materials.

Acknowledgments

This study was supported by National Natural Science Foundation of China (Grant Nos. 11505121 and 11775150). We appreciate the supports from Key Laboratory of Nuclear Materials and Safety Assessment (2017NMSAKF02).

References

[1] M.C. Troparevsky, J.R. Morris, M. Daene, Y. Wang, A.R. Lupini, G.M. Stocks, JOM 67 (2015) 2350–2363.
[2] Y. Zhang, T.T. Zuo, Z. Tang, M.C. Gao, K.A. Dahmen, P.K. Liaw, Z.P. Lu, Prog. Mater. Sci. 61 (2014) 1–93.
[3] N.A.P.K. Kumar, C. Li, K.J. Leonard, H. Bei, S.J. Zinkle, Acta Mater. 113 (2016) 230–244.
[4] T. Yang, S. Xia, W. Guo, R. Hu, J.D. Poplawsky, G. Sha, Y. Fang, Z. Yan, C. Wang, C. Li, Y. Zhang, S.J. Zinkle, Y. Wang, Scr. Mater. 144 (2018) 31–35.
[5] C. Lu, L. Niu, N. Chen, K. Jin, T. Yang, P. Xiu, Y. Zhang, F. Gao, H. Bei, S. Shi, M.-R. He, I.M. Robertson, W.J. Weber, L. Wang, Nat. Commun. 7 (2016), 13564. .
[6] S.Q. Xia, X. Yang, T.F. Yang, S. Liu, Y. Zhang, JOM 67 (2015) 2340–2344.
[7] C. Lu, T. Yang, K. Jin, N. Gao, P. Xiu, Y. Zhang, F. Gao, H. Bei, W.J. Weber, K. Sun, Y. Dong, L. Wang, Acta Mater. 127 (2017) 98–107.
[8] M.-R. He, S. Wang, S. Shi, K. Jin, H. Bei, K. Yasuda, S. Matsumura, K. Higashida, I.M. Robertson, Acta Mater. 126 (2017) 182–193.
[9] G.S. Was, Fundamentals of Radiation Materials Science, SpringerNature, New York 2017, pp. 255–299.
[10] G.S. Was, (2017).
[11] X. Lin, Q. Peng, E.-H. Han, W. Ke, C. Sun, Z. Jiao, Scr. Mater. 149 (2018) 11–15.
[12] A.J. Ardell, P. Bellon, Curr. Opinion Solid State Mater. Sci. 20 (2016) 115–139.
[13] O.K. Chopra, A.S. Rao, J. Nucl. Mater. 409 (2011) 235–256.
[14] E.A. Kenik, J.T. Busby, Mater. Sci. Eng. R. Rep. 73 (2012) 67–83.
[15] A.D. Marwick, Journal of Physics F: Metal Physics 8 (1978) 1849.
[16] P.R. Okamoto, J. Nucl. Mater. 53 (1974) 336–345.
[17] R.P. Doerner, Scr. Mater. 143 (2018) 137–141.
[18] N. MATSUNAMI, Atomic Data and Nuclear Data 31 (1984) 1–80.
[19] R.P. Doerner, D. Nishijima, T. Schwarz-Selinger, Phys. Scr. T159 (2014), 014040. .
[20] S. Kajita, T. Yoshida, D. Kitaoka, R. Etoh, M. Yajima, N. Ohno, H. Yoshida, N. Yoshida, Y. Terao, J. Appl. Phys. 113 (2013), 134301. .
[21] Y. Lao, W. Niu, Y. Shi, H. Du, H. Zhang, S. Hu, Y. Wang, J. Alloys Compd. 739 (2018) 401–406.
[22] I.J. Beyerlein, M.J. Demkowicz, A. Misra, B.P. Uberuaga, Prog. Mater. Sci. 74 (2015) 125–210.
[23] C.H.S.A.N. Koga, J. Phys. Chem. A 105 (2001) 5940–5944.
[24] A. Janotti, M. Krcmar, C.L. Fu, R.C. Reed, Phys. Rev. Lett. 92 (2004), 085901. .
[25] M.E. Glicksman, Diffusion in Solids: Field Theory, Solid State Principles and Applications, John Wiley, New York, 1999.
[26] K.Y. Tsai, M.H. Tsai, J.W. Yeh, Acta Mater. 61 (2013) 4887–4897.